Molecular Immunology 108 (2019) 111–120

Contents lists available at ScienceDirect

Molecular Immunology

journal homepage: www.elsevier.com/locate/molimm

The ubiquitin-like modifier FAT10 is required for normal IFN-γ production by activated CD8$^+$ T cells

Mei Min Mah[a], Michael Basler[a,b], Marcus Groettrup[a,b,*]

[a] Division of Immunology, Department of Biology, University of Konstanz, 78457 Konstanz, Germany
[b] Biotechnology Institute Thurgau at the University of Konstanz, 8280 Kreuzlingen, Switzerland

ARTICLE INFO

Keywords:
FAT10
Ubiquitin-like modifier
LCMV
IAV
Interferon response

ABSTRACT

FAT10 is the only ubiquitin-like modifier which directly targets its substrate proteins for rapid degradation by the proteasome. While the conjugation and proteasomal targeting of FAT10 are fairly well understood, the biological functions of FAT10 have remained largely elusive. Here we have investigated the role of FAT10 in cytokine responses in mice upon viral infection. We used lymphocytic choriomeningitis virus (LCMV) infection of mice to induce the IFN-γ and TNF-α-dependent expression of FAT10. We found that TCR-stimulated splenocytes derived from LCMV-infected FAT10$^{-/-}$ mice secreted less IFN-γ and expressed less mRNA for IL-12 p40 but secreted more IFN-α and IFN-β compared to FAT10$^{+/-}$ mice. The reduction in IFN-γ secretion could be assigned to CD8$^+$ T cells. Nevertheless, LCMV viral clearance was similar in FAT10$^{-/-}$ as compared to FAT10$^{+/-}$ mice. Since FAT10 has previously been reported to promote influenza A virus (IAV) replication *in vitro* we have studied the effect of FAT10 deficiency during IAV infection in mice. Unexpectedly, IAV titers and disease symptoms were not changed in FAT10$^{-/-}$ mice even though the *Fat10* mRNA was rapidly induced in the lung upon IAV infection. In conclusion, we find that FAT10 fine-tunes the balance of interferons during viral infection by lowering the production of type I and enhancing type II interferons.

1. Introduction

FAT10 is a ubiquitin-like protein that was discovered by chromosomal sequencing in an effort to identify additional genes from the human major histocompatibility complex (MHC). Since FAT10 is encoded in the MHC locus, it received its name according to its proximity to the HLA-F locus as HLA-F adjacent transcript 10 (FAT10) (Fan et al., 1996) and has also been designated ubiquitin D (UBD). FAT10 is an 18 kDa protein which is made up of 165 amino acids having a short half-life of one hour (Hipp et al., 2005; Raasi et al., 2001). FAT10 consists of two ubiquitin-like domains which are joined by a short linker of five amino acids. The two N- and C-terminal ubiquitin-like domains of FAT10 share 29% and 36% sequence identity to ubiquitin, respectively. In contrast to ubiquitin that requires post-translational cleavage to expose its terminal diglycine motif, the FAT10 protein is synthesized with an accessible diglycine motif at its very C-terminus (Bates et al., 1997). The diglycine motif is essential for the isopeptide linkage of FAT10 to hundreds of different substrates, a process termed FAT10ylation (Aichem et al., 2012; Raasi et al., 2001). FAT10ylation is mediated by an E1, E2, and possibly an E3 enzyme cascade. In this process, UBA6 (referred to as UBE1L2, E1-L2, or MOP-4) (Jin et al., 2007; Pelzer et al., 2007) and USE1 (UBA6-specific E2 enzyme) (Aichem et al., 2010) serve as the E1-type activating and E2-type conjugating enzymes, respectively. FAT10 has been found to play a role in various cellular processes, like apoptosis (Liu et al., 1999; Raasi et al., 2001; Ross et al., 2006), spindle checkpoint control during mitotic cell cycle (Liu et al., 1999; Merbl et al., 2013; Ren et al., 2006, 2011), and NF-κB activation (Gong et al., 2010). Notably, FAT10 is highly expressed in a dozen of different human tumors (Aichem and Groettrup, 2016).

Several studies showed the importance of FAT10 in the immune system. First, the basal expression of *fat10* mRNA is primarily found in organs of the immune system, *e.g.* thymus, fetal liver, lymph nodes, and spleen (Canaan et al., 2006; Lee et al., 2003; Lukasiak et al., 2008). Second, FAT10 expression is found to be synergistically induced by the pro-inflammatory cytokines, IFN-γ and TNF-α (Choi et al., 2014; Liu et al., 1999; Raasi et al., 1999). This was recently confirmed for various immune cell subsets of mouse and human origin (Schregle et al., 2018).

Abbreviations: FAT10, HLA-F adjacent transcript 10; IAV, influenza A virus; LCMV, lymphocytic choriomeningitis virus; MEF, mouse embryonic fibroblasts; RIG-I, retinoic acid-inducible gene I

* Corresponding author at: Division of Immunology, Department of Biology, University of Konstanz, Universitaetsstrasse 10, D-78457 Konstanz, Germany.
E-mail address: Marcus.Groettrup@uni-konstanz.de (M. Groettrup).

https://doi.org/10.1016/j.molimm.2019.02.010
Received 13 October 2018; Received in revised form 18 January 2019; Accepted 13 February 2019
Available online 25 February 2019

Third, FAT10 becomes up-regulated upon maturation of dendritic cells (Bates et al., 1997), which are considered to be the only antigen presenting cells (APCs) that are able to prime naïve $CD8^+$ T cells upon viral infection (den Haan et al., 2000). Fourth, mice lacking FAT10 demonstrated hypersensitivity towards endotoxin challenge by lipopolysaccharides (LPS) (Canaan et al., 2006). Fifth, FAT10 was involved in the defense against intracellular bacteria by decorating *Salmonella typhimurium* targeted for autophagy (Spinnenhirn et al., 2014). Moreover, FAT10 has been shown to play a role in viral replication by interfering with the RIG-I signaling pathways. It was observed that FAT10 up-regulation following H5N1 influenza A virus infection *in vitro* promoted H5N1 viral replication through the inhibition of type I interferons (IFNs), thus reducing the viability of infected cells (Zhang et al., 2016).

Lymphocytic choriomeningitis virus (LCMV) is one of the most commonly used mouse model systems to study the antiviral immune response and viral persistence (Oldstone et al., 1985). It is well established that upon LCMV infection, IFN-γ is produced by activated T cells, including $CD4^+$ T helper cell type 1 (Th1) lymphocytes and $CD8^+$ cytotoxic T lymphocytes, as well as natural killer (NK) cells (Kägi et al., 1994; Orange and Biron, 1996). In the early stage during infection, NK cells are responsible for immediate IFN-γ secretion. At a later time during the adaptive immune response, T lymphocytes will act as the prime secretors of IFN-γ (Frucht et al., 2001; Sen, 2001). In this study, the role of FAT10 in T cell immunity to viral infection is addressed, by assessing an acute infection of $FAT10^{-/-}$ mice with LCMV and IAV. In our study, we show that $FAT10^{-/-}$ mice manifested an altered cytokine response with regard to type I and type II interferon secretion upon LCMV infection, suggesting the involvement of FAT10 in the antiviral immune response.

2. Materials and methods

2.1. Mice

C57BL/6 mice (H-2b) were originally purchased from Charles River, Germany. FAT10-deficient ($FAT10^{-/-}$) mice were kindly provided by A. Canaan and S.M. Weissman (Yale University School of Medicine, New Haven, USA) (Canaan et al., 2014) and backcrossed onto C57BL/6 background for at least 10 generations. $FAT10^{+/-}$ mice were generated by crossing C57BL/6 and $FAT10^{-/-}$ mice. 8–10 week old mice were used for all experiments. Animal experiments were approved by the Review Board of Governmental Presidium Freiburg of the State of Baden-Württemberg, Germany.

2.2. Infection

Age- and sex-matched mice were infected intravenously (i.v.) with 200 pfu LCMV-WE and propagated on the fibroblast cell line L929. For infection with influenza A virus, age- and sex-matched mice were anesthetized with isofluorane and infected intranasally (i.n.) with influenza virus strain A/Regensburg/D6/09 (H1N1pdm09, RB1) at $10 \times 50\%$ of a mouse lethal dose (MLD_{50}) ($10 \times MLD_{50} = 5 \times 10^4$ pfu). The weight of the mice was monitored daily and mice were euthanized at the clinical end point of 75% of the initial bodyweight.

2.3. Generation of mouse embryonic fibroblast (MEFs)

The preparation of MEFs was performed as previously described (Bitzer et al., 2017).

2.4. Peripheral blood mononuclear cell (PBMC) isolation

Blood donations for research purposes were approved by the Ethics Committee of Konstanz University, and individual donors gave written consent. PBMCs from healthy donors were enriched by density gradient centrifugation on Ficoll-Paque™ Plus (GE Healthcare, Germany).

2.5. MACS sorting

$CD3^+$, $CD4^+$, $CD8^+$, $CD19^+$ and pan T cell purification was performed by MACS in accordance with the manufacturer's protocols (Miltenyi Biotec). The purity of the MACS sorted cells was determined by flow cytometry (Accuri® C6 flow cytometry, USA).

2.6. In vitro T-cell stimulation and cell culture

Splenocytes from C57BL/6, $FAT10^{+/-}$ and $FAT10^{-/-}$ mice were stimulated *in vitro* with 5 µg/ml plate-bound anti-CD3ε (145-2C11) and anti-CD28 (37.51) and cultured for 24 h in IMDM supplemented with 10% FCS, 0.1% β-ME and 100 U/mL penicillin/streptomycin. Media and supplements were purchased from Invitrogen-Life Technologies. C57BL/6 MEFs and the sorted immune cell subsets from mice or PBMCs were stimulated with the following cytokines: 400 U/mL TNF-α, 200 U/mL IFN-γ, 400 U/mL IL-6 (all from PeproTech), 200 U/mL IFN-α (BioLegend) and 1000 U/mL IFN-β (PBL Assay Science) for 24 h unless otherwise stated.

2.7. ELISA

Supernatants from cultured cells or sera were collected at the indicated time points. Cytokines were analyzed by ELISA kits (IFN-γ: ThermoFischer, IFN-α: PBL Assay Science, IFN-β: BioLegend) according to the manufacturers' instructions.

2.8. Real-time RT-PCR

RNA was purified using the RNeasy® Plus Mini Kit (Qiagen, Germany) according to the manufacturer's instructions. For synthesis of single-stranded cDNA from total RNA, the Reverse Transcription System (Promega, Germany) was used. Gene expression was measured by TOptical Gradient 96 Real-Time PCR-Thermocycler and the qPCRsoft V3.1 software (both from Analytik Jena, Germany), with the

Table 1
Primer pairs for quantitative RT-PCR.

mRNA	Forward (5′ to 3′)	Reverse (5′ to 3′)
(MOUSE) fat10	GGGATTGACAAGGAAACCACTA	TTCACAACCTGCTTCTTAGGG
(MOUSE) ifn-γ	TGA ACG CTA CAC ACT GCA TCT TGG	CGA CTC CTT TTC CGC TTC CTG AG
(MOUSE) il-12 p35	AACT TTGGCATTGTGGAAGG	ACACATTGGGGGTAGGAACA
(MOUSE) il-12 p40	CAGAAGCTAACCATCTCCTGGTTTG	TCCGGAGTAATTTGGTG CTTCACAC
(MOUSE) rpl13a	TGAAGGCATCAACATTTCTGG	GGTAAGCAAACTTTCTGGTAG
(MOUSE) gapdh	GTGTTCCTACCCCCAATGT	TGTCATCATACTTGGCAGGTTTC
(MOUSE) β-act	GACCTCTATGCCAACACAGT	ACTCATCGTACTCCTGCTTG
(MOUSE) mx1	CCTGGAGGAGCAGAGTGACAC	GGTTAATCGGAGAATTTGGCAA
(MOUSE) hprt	CCAGCAGGTCAGCAAAGAACTTA	TGGACAGGACTGAAAGACTTG
(HUMAN) Fat10	CTGTGTGCATGTCCGTTCCGA	GGGTAAGGTGGATGGTCTTCTCT
(HUMAN) Rpl13a	CTACAGAAACAAGTTGAAGTACCTG	ATGCCGTCAAACACCTTGAG

following primers listed in Table 1.

Relative gene expression was calculated using the Excel-based relative expressions software tool (REST©) according to the Pfaffl method (Pfaffl et al., 2002). mRNA expression levels are shown as arbitrary units (AU) of real-time RT-PCR data.

2.9. Focus forming assay for LCMV viral load

Titers of LCMV in spleens of i.v.-infected mice were determined on adherent fibroblasts cells (MC57) as previously described (Basler et al., 2009).

2.10. Influenza virus plaque assay

Titers of IAV in the lungs of i.n.-infected mice were determined on Madin Darby canine kidney (MDCK II) cells as previously described (Herrmann et al., 2015).

2.11. Flow cytometry and intracellular cytokine staining (ICS)

Single-cell suspensions were prepared from spleen through mechanical disruption of tissues and were centrifuged at 1500 rpm for 90 s. Supernatants were discarded and cells were stained with the following antibodies: APC-conjugated anti-CD3 (17A2), PE-conjugated anti-CD4 (GK1.5), PE-conjugated anti-NK1.1 (PK136), FITC-conjugated anti-CD11c (N418), FITC-conjugated anti-Ly-6G (RB6-8C5) which were purchased from ThermoFischer, USA. FITC-conjugated anti-CD8 (53-6.7), APC-conjugated anti-CD19 (1D3), APC-conjugated anti-CD11b (M1/70), PE-conjugated anti-CD90.2 (53-2.1) were purchased from BD Biosciences. For intracellular cytokine staining following LCMV infection, splenocytes were stimulated *in vitro* with 5 µg/ml of plate-bound anti-CD3ε (145-2C11) and anti-CD28 (37.51) for 19 h at 37 °C, followed by 10 µM/ml brefeldin A (Sigma Aldrich) for 5 h at 37 °C. Then, cells were surface stained with PE-conjugated anti-CD4 (GK1.5) and APC-conjugated anti-CD8 (53-6.7), fixed, permeabilized, and stained intracellularly for FITC-conjugated anti-IFN-γ (XMG1.2). Samples were analyzed using FACSVerse (BD Biosciences) and FlowJo (ThreeStar Inc, Ashland, OR, USA) software.

2.12. Statistical analysis

For statistical analyses, groups from similar experiments were pooled and analyzed for significant differences as indicated in the graph. All statistical analyses were performed using GraphPad Prism software (version 6.04) (GraphPad, San Diego, CA).

3. Results

3.1. Fat10 mRNA becomes up-regulated upon LCMV infection

Previous studies have found higher expression of FAT10 in lymphoid organs, such as thymus, spleen, lymph nodes and fetal liver (Canaan et al., 2006; Lee et al., 2003; Lukasiak et al., 2008). To examine whether LCMV infection can lead to induction of the *fat10* gene, WT mice were infected with LCMV-WE for either 3 days or 8 days. Quantitative real-time RT-PCR analysis was performed on total spleen and thymus, as well as magnetically purified $CD4^+$, $CD8^+$ and $CD19^+$ cells (purity: over 85%) from the spleen (Fig. 1). Compared to naive mice, *fat10* mRNA expression in $CD4^+$ T cells was significantly induced on day 3 post LCMV infection and was not further increased on day 8 post infection (Fig. 1C). In the thymus and in $CD19^+$ B cells, a significantly elevated *fat10* mRNA expression could only be observed on day 8 post infection (Fig. 1B and E), while LCMV infection led to a gradual increase in *fat10* gene expression in the spleen and in $CD8^+$ T cells (Fig. 1A and D). These results suggest that LCMV infection leads to overall *fat10* mRNA induction, with early (3 days post LCMV infection) and late (8 days post LCMV infection) expression depending on the type of immune cell or organ.

3.2. Reduced IFN-γ production in LCMV infected $FAT10^{-/-}$ mice

IFN-γ is an important pro-inflammatory cytokine for the early and late defence against LCMV (Ou et al., 2001; van den Broek et al., 1995). Since FAT10 silencing has caused an elevation of the type I interferon response upon virus infection *in vitro* (Zhang et al., 2016) and since IFN-α/β downregulate IFN-γ production, we have investigated whether FAT10 deficiency in LCMV-infected mice would affect the IFN-γ response. FAT10 is strongly induced in $CD4^+$ and $CD8^+$ cells on day 3 post LCMV infection (Fig. 1). Therefore, splenocytes from LCMV infected WT, $FAT10^{+/-}$ and $FAT10^{-/-}$ mice (3 days post infection) were stimulated *in vitro* with plate bound αCD3ε/αCD28 antibodies and IFN-γ secretion into the supernatant was assessed. No difference in IFN-γ concentrations in the supernatant of splenocytes between uninfected WT and $FAT10^{+/-}$ mice compared to $FAT10^{-/-}$ mice was found (Fig. 2A). In contrast, on 3 days post LCMV infection, when FAT10 is strongly induced (Fig. 1), splenocytes of $FAT10^{-/-}$ mice secreted about 50% less IFN-γ (Fig. 2B). This was further confirmed by the assessment of mRNA expression levels of *ifn-γ* in splenocytes of LCMV infected $FAT10^{-/-}$ mice (3 days post infection) (Fig. 2D). However, no differences in IFN-γ level could be observed in the serum on day 3 or day 4 post LCMV infection (Fig. 2C).

T cells are the major producers of IFN-γ during LCMV infection (Huang et al., 1993). To test whether T cells contribute to reduced IFN-γ production in $FAT10^{-/-}$ mice, we assessed intracellular IFN-γ production of $CD4^+$ and $CD8^+$ cells from LCMV infected (day 3) $FAT10^{+/-}$ and $FAT10^{-/-}$ mice. Splenocytes of mice were stimulated *in vitro* with plate bound αCD3ε/CD28 antibodies for 24 h and IFN-γ was stained intracellularly. $CD8^+$ cells from splenocytes of $FAT10^{-/-}$ mice secreted less IFN-γ compared to $FAT10^{+/-}$ mice whereas no difference was seen for $CD4^+$ cells (Fig. 2E). Thus, reduced IFN-γ secretion observed in TCR-stimulated $FAT10^{-/-}$ splenocytes (Fig. 2B) can be assigned at least in part to $CD8^+$ T cells.

IL-12 produced by monocytes, dendritic cells and macrophages leads to the differentiation of naïve T cells into Th1 cells and stimulates the production of IFN-γ of T cells *via* STAT-4 signalling (Suarez-Ramirez et al., 2014). Since IL-12 could not be detected in the supernatant of TCR-stimulated LCMV infected splenocytes, real-time RT-PCR was performed to determine the gene expression level of *il-12* for its subunits, p35 and p40. Splenocytes of $FAT10^{-/-}$ mice showed significantly less mRNA expression for the IL-12 p40 subunit but no difference for the IL-12 p35 subunit in comparison to $FAT10^{+/-}$ mice (Fig. 2F). A reduced IL-12 p40 expression can account for diminished IFN-γ production in the absence of FAT10.

Next, we wanted to examine whether reduced IFN-γ secretion from splenocytes of $FAT10^{-/-}$ mice could be attributed to a change of cell type composition. Thus, different lymphocyte sub-populations (CD3, CD4, CD8, CD19, NK1.1, CD11c and CD90.2) in the spleen of naïve or LCMV-infected (day 3 post infection) $FAT10^{+/-}$ and $FAT10^{-/-}$ mice were analyzed (Fig. S1). No significant differences in the composition and absolute cell number of lymphocyte sub-populations were observed in uninfected (naïve) (Fig. S1A) or LCMV-infected mice (Fig. S1B).

3.3. Increased type I interferon secretion by LCMV infected $FAT10^{-/-}$ mice

IFN-α/IFN-β were shown to negatively regulate IFN-γ expression of natural killer cells and T cells (Nguyen et al., 2000). Having demonstrated the reduced IFN-γ expression in $FAT10^{-/-}$ splenocytes (Fig. 2B), we next asked whether $FAT10^{-/-}$ mice could secrete more type I IFNs as a means to control the viral infection. Thus, $FAT10^{+/-}$ and $FAT10^{-/-}$ mice were infected with LCMV and IFN-α and IFN-β production in the spleen and serum were analyzed on day 3 post

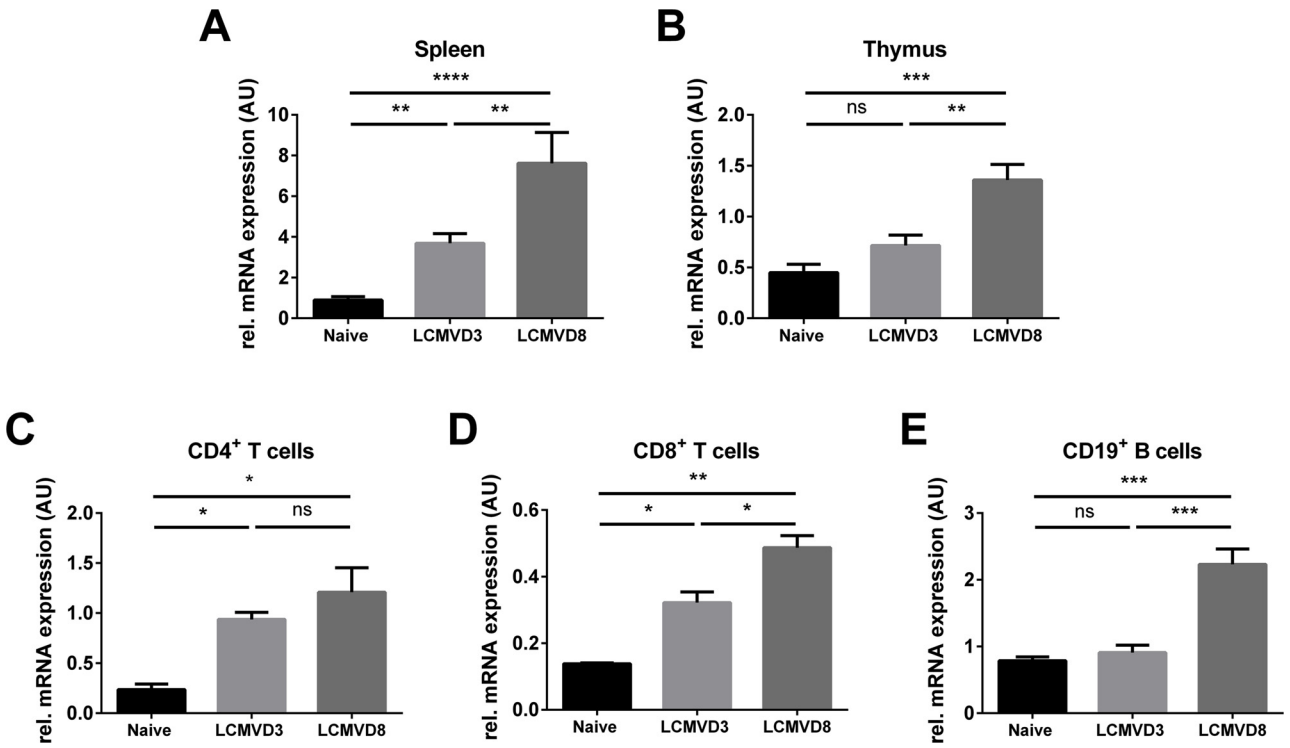

Fig. 1. LCMV-WE induced *fat10* mRNA expression. Quantification of *fat10* mRNA levels in C57BL/6 mice without (naive) or with LCMV-WE infection for either 3 days (LCMV-D3) or 8 days (LCMV-D8). *Fat10* mRNA expression was determined by real-time RT-PCR and normalized to *rpl13a*. The relative mRNA expression was calculated with the value for naive being arbitrarily set to unity. *Fat10* gene expression in spleen (**A**) and thymus (**B**) of C57BL/6 mice is shown. Splenocytes of C57BL/6 naïve, LCMV-D3 or LCMV-D8 infected mice were magnetically sorted for $CD4^+$ T cells (**C**), $CD8^+$ T cells (**D**) and $CD19^+$ B cells (**E**). *p < 0.05; **p < 0.01; *** p < 0.005; ****p < 0.001; ns, statistically not significant by one-way ANOVA Tukey's multiple comparisons test. Values represent mean ± SEM. The experiments were repeated for at least three times with similar outcomes.

infection. Significantly higher IFN-α and IFN-β secretion from splenocytes of $FAT10^{-/-}$ mice compared to their heterozygous littermates were found (Fig. 3A and B). Although reduced IFN-γ levels in $FAT10^{-/-}$ mice were not detectable in the serum (Fig. 2C), type I IFNs were increased in the serum of $FAT10^{-/-}$ mice (Fig. 3C and D) with IFN-α but not yet IFN-β levels reaching statistical significance (Fig. 3D). Additionally, immune cell subsets like $CD4^+$ T cells, $CD8^+$ T cells and $CD19^+$ B cells were magnetically sorted from LCMV infected mice to detect IFN-α secretion in the supernatant after incubation for 24 h. $CD4^+$ T cells and $CD19^+$ B cells but not $CD8^+$ T cells showed a significantly higher secretion of IFN-α (Fig. 2E). Taken together, our data showed that splenocytes, serum and certain immune cell subsets from $FAT10^{-/-}$ mice 3 days post LCMV infection secreted higher amounts of type I IFNs.

3.4. The efficacy of LCMV clearance in $FAT10^{-/-}$ mice is similar to that of $FAT10^{+/-}$ mice

During LCMV infection, IFN-γ secreted by natural killer cells and $CD8^+$ T cells is crucial for viral clearance (Orange and Biron, 1996). Since $FAT10^{-/-}$ splenocytes showed reduced IFN-γ secretion (Fig. 2B), we investigated the efficiency of LCMV viral clearance in $FAT10^{-/-}$ mice (Fig. 4). A similar viral burden as compared to $FAT10^{+/-}$ mice was measured in spleens of $FAT10^{-/-}$ mice on day 3 post infection. Since reduced IFN-γ secretion by $FAT10^{-/-}$ mice was detectable only on day 3 post LCMV infection, the effect in viral clearance might be visible at later time points of infection. However, no difference in viral titers could be found neither on day 4 nor on day 6 post infection when LCMV titers had already declined tenfold (Fig. 4). These data show that FAT10 is dispensable for LCMV clearance.

3.5. FAT10 deficiency doesn't affect symptoms, viral titers but alters the IFN-α response to influenza A virus

In vitro studies have shown that FAT10 promotes IAV replication by interfering with type I IFN secretion and reducing STAT1 phosphorylation (Zhang et al., 2016). Therefore, we assessed type I IFN and IFN-γ secretion in $FAT10^{+/-}$ and $FAT10^{-/-}$ mice infected intranasally with 10 x LD50 of influenza A virus (IAV) strain A/Regensburg/D6/09 (H1N1pdm09, RB1). Splenocytes and lung cells derived from IAV infected mice (day 2 and day 4) were incubated *in vitro* for 24 h at 37 °C without further stimulation. No differences in IFN-α, IFN-β and IFN-γ secretion from splenocytes and lung cells of $FAT10^{-/-}$ mice compared to $FAT10^{+/-}$ mice were detected on day 2 and day 4 post IAV infection (Fig. 5A–C). Serum collected from $FAT10^{-/-}$ mice contained significantly less IFN-α compared to $FAT10^{+/-}$ mice on day 2 post IAV infection, followed by a significantly higher IFN-α content on day 4 post IAV infection (Fig. 5D). However, the IAV titers in the lung of $FAT10^{+/-}$ and $FAT10^{-/-}$ mice on day 2 and day 4 after infection showed no differences (Fig. 5E). Next, the susceptibility of $FAT10^{+/-}$ and $FAT10^{-/-}$ mice to IAV was investigated. The body weight of the mice was monitored daily and mice were euthanized when weight loss reached 25% of their initial body weight. $FAT10^{+/-}$ and $FAT10^{-/-}$ mice exhibited comparable weight loss (Fig. 5F). All mice had reached the clinical end point by day 12 post IAV infection (Fig. 5F). It was reported that *Fat10* mRNA was up-regulated following H5N1 influenza A virus infection in A549 cells *in vitro* (Zhang et al., 2016). This prompted us to investigate whether IAV infection would lead to FAT10 up-regulation in the lung of the infected mice. *Fat10* mRNA was up-regulated in mice infected with IAV, starting from day 1 till day 4 post infection as compared to the uninfected mice, with a maximum of *fat10* mRNA expression found on day 2 post IAV infection (Fig. 5G). Collectively, these data showed that even though FAT10 was markedly up-

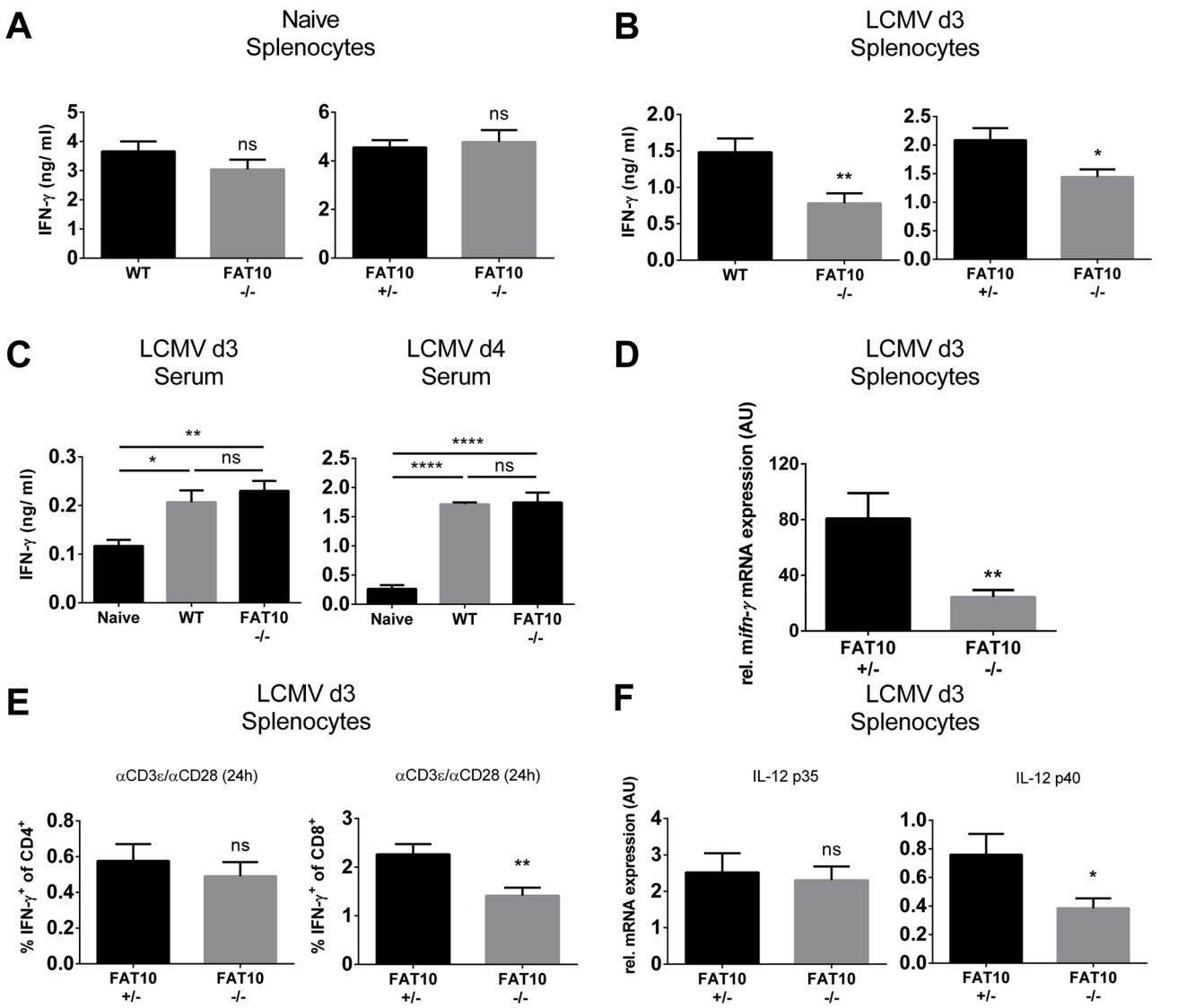

Fig. 2. Reduced IFN-γ production in splenocytes of LCMV-WE infected FAT10$^{-/-}$ mice. Splenocytes of uninfected (naive) mice (**A**) or mice infected with LCMV-WE for 3 days (LCMV d3) (**B**) were stimulated overnight with plate bound αCD3ε/αCD28 antibodies and IFN-γ in the supernatant was determined by ELISA. (**C**) Mice were infected with LCMV-WE for 72 h (LCMV d3) and for 96 h (LCMV d4). IFN-γ levels in the serum were measured by ELISA. The control (Naive) represents WT mice without LCMV-WE infection. (**D**) Quantification of *ifn*-γ mRNA expression levels from splenocytes of mice infected with LCMV-WE (day 3) and stimulated overnight with plate bound αCD3ε/αCD28 antibodies. *Ifn*-γ mRNA expression was determined by real-time RT-PCR and normalized to *rpl13a*. The relative mRNA expression was calculated with the value for unstimulated cells being arbitrarily set to unity. (**E**) Splenocytes of mice infected with LCMV-WE (day 3) were stimulated overnight with plate bound αCD3ε/αCD28 antibodies and intracellular cytokine stainings (ICS) for IFN-γ of CD4$^+$ and CD8$^+$ cells were analyzed by flow cytometry. (**F**) Quantification of *il-12* mRNA levels from splenocytes of mice infected with LCMV-WE (day 3) and stimulated overnight with plate bound αCD3ε/αCD28 antibodies. mRNA expression for IL-12 subunits p35 (left) and p40 (right) was determined by real-time RT-PCR and normalized to *rpl13a*. The relative mRNA expression was calculated with the value for unstimulated being arbitrarily set to unity *p < 0.05; **p < 0.01; ***p < 0.005; ****p < 0.0001; ns, statistically not significant by Student's *t*-test except for (C). (C) is analyzed by one-way ANOVA Tukey's multiple comparisons test. Error bars represent mean ± SEM. [n = 20 from 5 independent experiments for (A), n = 25 from 6 independent experiments for (B), n = 5 from 2 independent experiments for (C), n = 9 from 3 independent experiments for (D), n = 8 from 2 independent experiments for (E) and n = 12 from 3 independent experiments for (F)].

regulated upon IAV infection, FAT10 deficiency did not affect the course of the disease.

3.6. The combination of TNF-α and IFN-γ is by far most potent in the induction of fat10 mRNA expression

Since *fat10* expression was induced quite early after i.n. IAV infection (Fig. 5G), we were interested to compare type I and type II IFNs and the combination of them with TNF-α with respect to their ability to enhance *fat10* mRNA expression. C57BL/6 MEFs were stimulated for 24 h with the respective cytokines alone and in combination. Real time RT-PCR analysis revealed that sole IFN-γ stimulation showed the highest *fat10* mRNA induction when compared with single stimulations with IFN-α, IFN-β and TNF-α. A joined treatment with TNF-α and IFN-γ achieved by far the highest *fat10* mRNA expression when compared with combination of TNF-α/IFN-α and TNF-α/IFN-β (Fig. 6A). Real-time RT-PCR analysis of the mRNA of the *mx1* gene, which is a known interferon inducible gene, was assessed to ascertain the functionality of the type I interferons used (Fig. S2A). Recently, joint stimulation of TNF-α and IL-6 in HepG2 cells was reported to up-regulate *Fat10* mRNA expression (Choi et al., 2014). Thus, we decided to quantitatively compare the potency of combinations of TNF-α/IFN-γ with TNF-α/IL-6 for *Fat10* mRNA induction in T cells and B cells magnetically sorted from both mouse splenocytes and human PBMCs. The purity of the

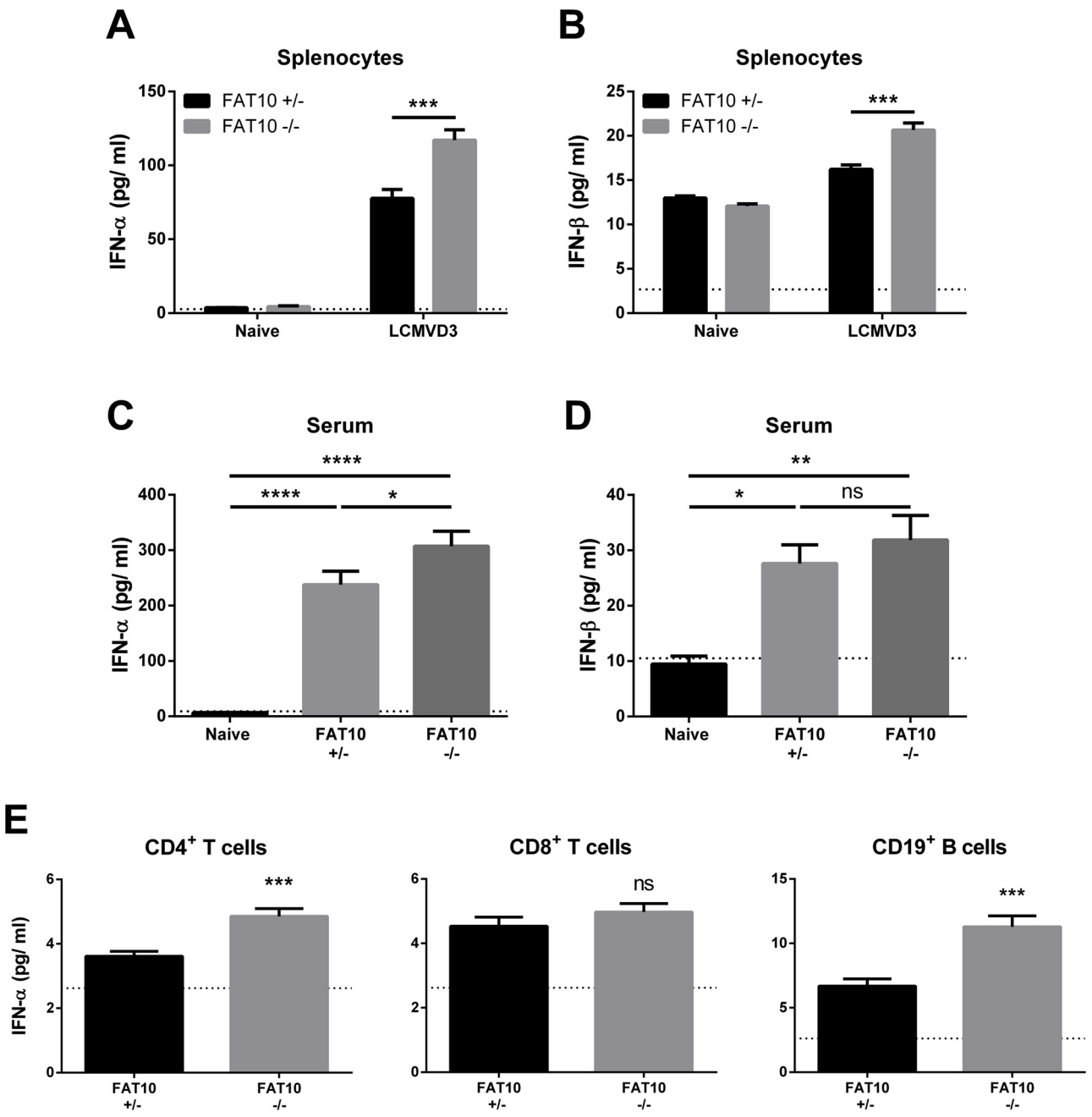

Fig. 3. Increased type I IFN levels in LCMV-WE infected FAT10$^{-/-}$ mice. Splenocytes from FAT10$^{+/-}$ and FAT10$^{-/-}$ mice infected with LCMV-WE for 72 h were cultured without stimulation. IFN-α (**A**) and IFN-β (**B**) from supernatants were measured after a 24 h culture by ELISA. IFN-α (**C**) and IFN-β (**D**) in the serum of these mice were measured by ELISA. (**E**) Splenocytes of LCMV day3 infected mice were magnetically sorted for CD4$^+$ T cells, CD8$^+$ T cells and CD19$^+$ B cells. IFN-α from supernatants were measured after a 24 h culture period without stimulation by ELISA. Dotted lines on graphs represent the detection limit of the ELISA. Naive represents uninfected mice. *** $p < 0.005$; ns, statistically not significant by Student's *t*-test for (A), (B) and (E). *$p < 0.05$; **$p < 0.01$; ****$p < 0.001$; ns, statistically not significant by one-way ANOVA Tukey's multiple comparisons test for (C) and (D). Values represent mean ± SEM. [n = 12 per group from 3 independent experiments for all experiments].

magnetically sorted cells was over 90% for all preparations. Unexpectedly, while TNF-α/IFN-γ strongly induced *fat10* mRNA in mouse and human B and T cells, we found no significant induction of *fat10* by TNF-α/IL-6 except for a twofold enhancement in CD3$^+$ mouse splenocytes (Fig. 6B and C). Next, a kinetic study of *Fat10* mRNA induction in T cells and B cells from human PBMCs with TNF-α/IL-6 treatment was performed. *Fat10* mRNA levels in human pan T cells and CD19$^+$ human B cells were first down-regulated and then slightly up-regulated at 24 h post TNF-α/IL-6 treatment thus indicating that also at earlier time points after TNF-α/IL-6 stimulation no transient up-regulation occurred (Fig. 6D). This weak stimulation by TNF-α/IL-6 was not due to a failure of the used IL-6 to activate the IL-6R because single stimulation of mouse splenocytes or human PBMCs with IL-6 (400 U/ml) readily induced IL-6-dependent STAT3 phosphorylation (Fig. S2B). These results indicate that FAT10 expression can be much more efficiently induced by a combined treatment with TNF-α and IFN-γ as compared to joint TNF-α/IL-6 stimulation.

4. Discussion

The profile of cytokines secreted by immune cells upon viral infections serves as a cornerstone of the immune response and is crucial

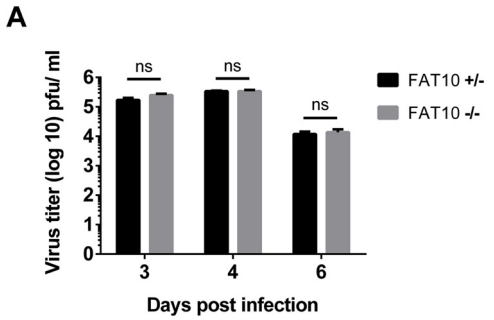

Fig. 4. Similar LCMV titers in FAT10$^{+/-}$ and FAT10$^{-/-}$ mice. (A) LCMV titers in the spleens of FAT10$^{+/-}$ and FAT10$^{-/-}$ mice infected with LCMV-WE for 3, 4 and 6 days. ns, statistically not significant by Student's *t*-test. Values represent mean ± SEM. [n = 12 per group from 3 independent experiments for all experiments].

for controlling acute infections. The major cytokines that are secreted upon LCMV infection include interferons of type I (IFN-α and IFN-β) and type II (IFN-γ), tumor necrosis factor (TNF) and interleukin-2 (IL-2). The aim of this study was to assess the function of FAT10 in antiviral immune responses in an *in vivo* setting. The basal expression of FAT10 in most tissues is low or absent, but it is readily and synergistically inducible by the pro-inflammatory cytokines, IFN-γ and TNF-α (Liu et al., 1999; Lukasiak et al., 2008; Raasi et al., 1999; Schregle et al., 2018). In our experimental settings, we could demonstrate that *Fat10* mRNA was up-regulated upon LCMV (Fig. 1) and IAV infection (Fig. 5G). *Fat10* mRNA was elevated by day 3 post LCMV infection in the spleen, in CD4$^+$, and in CD8$^+$ T cells, of which CD8$^+$ T cells are crucial in the clearance of LCMV. Also in the thymus and CD19$^+$ B cells, high expressions of *fat10* mRNA could be observed on day 8 post LCMV infection. In contrast, BALB/c mice and the human respiratory epithelial cell lines A549 infected with IAV H5N1 showed highest FAT10 expression already by 24 h post infection, whereas C57BL/6 mice infected with IAV in our experimental set-up revealed a peak of FAT10 expression on day 2 post infection (Fig. 5G). It would have been of interest to also measure the induction of FAT10 protein in the organs and lymphocytes of virus infected mice, but unfortunately, according to our knowledge and experience there is no antibody available to date which is sensitive enough to detect endogenous mouse FAT10.

A key finding of our study is that splenocytes derived from LCMV infected FAT10$^{-/-}$ mice have an impaired ability to secrete IFN-γ (Fig. 2B). This reduction of IFN-γ production could be assigned to CD8$^+$

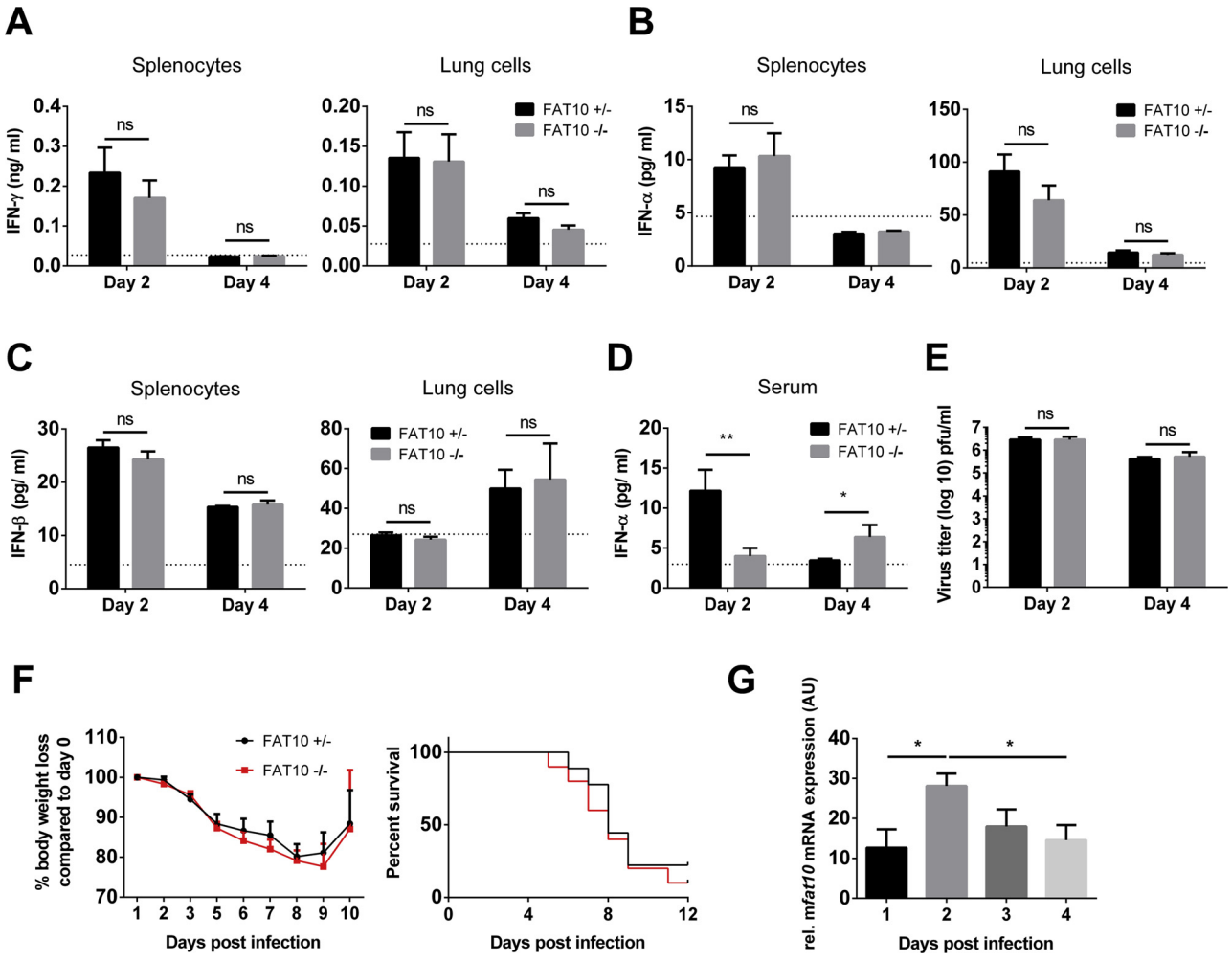

Fig. 5. Disease symptoms and interferon responses in IAV infected FAT10$^{-/-}$ mice. Splenocytes and lung cells from FAT10$^{+/-}$ and FAT10$^{-/-}$ mice infected with IAV for 48 h (Day 2) or 96 h (Day 4) were cultured overnight. Supernatants were collected and (**A**) IFN-γ, (**B**) IFN-α and (**C**) IFN-β levels were measured by ELISA. (**D**) Serum from FAT10$^{+/-}$ and FAT10$^{-/-}$ mice infected with IAV for 48 h (Day 2) or 96 h (Day 4) were collected and IFN-α levels were measured by ELISA. (**E**) IAV titers of FAT10$^{+/-}$ and FAT10$^{-/-}$ mice infected for 48 h (Day 2) or 96 h (Day 4) were determined. (**F**) The body weight and survival curve of FAT10$^{+/-}$ and FAT10$^{-/-}$ mice after IAV infection are shown. (**G**) *Fat10* mRNA expression from C57BL/6 lung was determined by real-time RT-PCR and normalized to GAPDH. *p < 0.05; **p < 0.01; ns, statistically not significant by Student's *t*-test. Values represent mean ± SEM. [n = 10 per group from 2 independent experiments on day 2 and n = 11 per group from 2 independent experiments on day 4].

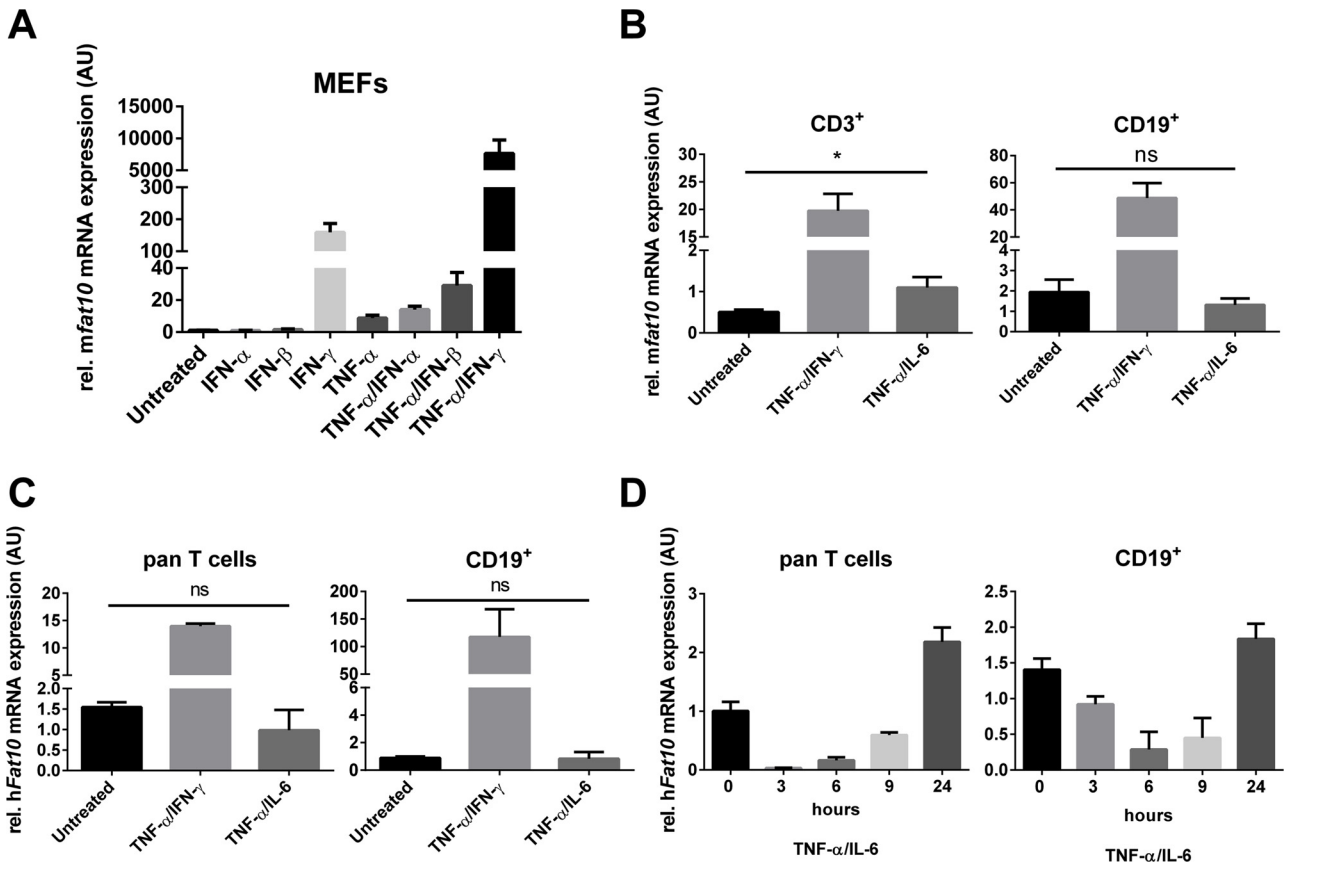

Fig. 6. The combined stimulation with TNF-α and IFN-γ leads to highest *Fat10* mRNA expression. Quantification of *Fat10* mRNA levels in (**A**) C57BL/6 MEFs, (**B**) C57BL/6 pan T and B cells (**C, D**) human PBMCs. The single immune cell subsets were magnetically sorted from splenocytes of mouse (B) or from PBMCs (**C, D**). Cells were left untreated or treated with indicated cytokines for either 24 h (A, B, C) or for indicated time periods (D). *Fat10* mRNA expression was determined by real-time RT-PCR and normalized to (A) *hprt*, (B) *β-actin* and (C, D) *rpl13a*. The relative mRNA expression was calculated with the value for untreated being arbitrarily set to unity. *p < 0.05 by Student's *t*-test. Values represent mean ± SEM. (n = 3 independent experiments).

T cells (Fig. 2E) which, in contrast to $CD4^+$ T cells, showed reduced IFN-γ content in intracellular IFN-γ staining experiments. In principle, also NK cells could contribute to the observed phenotype, but after one day stimulation of splenocytes with αCD3ε/αCD28 antibodies *in vitro*, NK cells did not persist under the employed culture conditions. IFN-γ plays a multifunctional role in the maintenance of the innate and adaptive immune response and is involved in the regulation of immune responses (Farrar and Schreiber, 1993). Despite showing reduced IFN-γ secretion (Fig. 2B), $FAT10^{-/-}$ mice displayed an unaltered competence as compared to $FAT10^{+/-}$ mice in clearing LCMV (Fig. 4). This might be due to the non-redundant role of ubiquitin and FAT10. Whereas FAT10 is expressed only under pro-inflammatory conditions, ubiquitin is expressed ubiquitously in all cell types (Canaan et al., 2006; Lee et al., 2003; Lukasiak et al., 2008). Both modifiers function as a protein signal for rapid degradation of substrate proteins through the proteasome. FAT10 shares many similarities to ubiquitin, both being equally efficient at targeting proteins for degradation (Schmidtke et al., 2014). Therefore, ubiquitin might have taken over the role of FAT10 in its absence, resulting in no differences in LCMV clearance in $FAT10^{-/-}$ mice.

Recently, Zhang et al. reported that recognition of the ssRNA of H5N1 IAV by the RNA helicases retinoic acid-inducible gene I (RIG-I) leads to enhanced FAT10 expression, promoting viral replication through suppression of type I IFNs secretion (Zhang et al., 2016). In that study, FAT10 knockdown in the lung epithelial cell line A549 and human bronchial epithelial cells reduced virus-induced cell death, while FAT10 overexpression by lentiviral transduction increased the replication of IAV. Overexpression of RIG-I and NF-kB p65 combined with using FAT10-Luc reporter plasmids in 293T cells confirmed that FAT10 up-regulation was mediated by RIG-I, leading to NF-κB activation. Furthermore, increased *Ifn-α* and *Ifn-β* mRNA levels were observed in A549 cells that were transfected with siRNA against FAT10 and subsequently infected with IAV strains H5N1 or H1N1 (Zhang et al., 2016).

This work had inspired us to look at IFN-α and IFN-β secretion in $FAT10^{-/-}$ mice post LCMV-WE infection. Indeed, we observed that $FAT10^{-/-}$ mice secreted more IFN-α and IFN-β in comparison to $FAT10^{+/-}$ mice on day 3 post LCMV infection (Fig. 3). This finding supports the observation made by Zhang *et al.*, and is in accordance with a report by Wilson et al., which demonstrates that blocking type I IFN signaling during persistent LCMV infection led to enhanced IFN-γ production. This allowed better control of the virus in LCMV-infected mice (Wilson et al., 2013). Similarly, Teijaro et al. reported that IFN-I blockade resulted in increased IFN-γ production 24 h post LCMV infection leading to reduced virus titers in mice (Teijaro et al., 2013). Even though we have seen increased type I IFNs and reduced IFN-γ production in LCMV-infected mice, these differences did not affect the ability of $FAT10^{-/-}$ mice to clear LCMV (Fig. 4). An attractive hypothesis for the function of FAT10 is that it might get conjugated to some virus-derived proteins thereby irreversibly targeting them for proteasomal degradation and slowing their rate of multiplication. This idea is in accordance with a late appearance of FAT10 in evolution possibly as a response to the emergence of a certain pathogen in mammals, given that FAT10 is only present in mammals and has evolved much later than the adaptive immune system. However, at least for the viruses tested in this study, FAT10 was not pivotal to

control their multiplication.

To use a second model of viral infection and to investigate the impact of FAT10 on IAV expansion *in vivo*, FAT10$^{-/-}$ mice were infected with influenza virus strain A/Regensburg/D6/09 (H1N1pdm09, RB1). No differences in the levels of type I and II interferons were detectable in the lungs of FAT10$^{-/-}$ and FAT10$^{+/-}$ mice on day 2 or day 4 post IAV infection (Fig. 5A–C). Consistently, IAV titers did not differ in the lungs of FAT10-deficient and proficient mice on day 2 and 4 post infection (Fig. 5E) and no effect of FAT10 deficiency on weight loss or survival after lethal IAV infection was observed (Fig. 5F). Similar to the reported FAT10 induction after IAV infection of human A549 cells *in vitro* (Zhang et al., 2016), FAT10 was readily induced in murine lungs after i.n. IAV infection *in vivo* (Fig. 5G and (Zhang et al., 2016)). However, it is unclear why the suppression of *Fat10* mRNA and protein in human A549 cells resulted in significantly reduced IAV replication and approximately two-fold enhanced IFN-α as well as IFN-β production by the infected A549 cells (Zhang et al., 2016). The observed *in vitro* effects may not be strong enough to affect interferon production and IAV replication *in vivo*. Alternatively, this discrepancy may reflect a species difference between the human and the mouse or the complex innate immune response in the mouse lung may overrule such differences. In any case, our *in vivo* data are not supporting the conception that FAT10 may be a promising drug target for pharmacologically ameliorating the course of an IAV infection.

Previously, it has been reported that joint stimulation of TNF-α and IL-6 leads to enhanced *Fat10* mRNA expression in HepG2 cells (Choi et al., 2014). The HepG2 cells were stimulated with 10 ng/ml of TNF-α and IL-6 for different time periods and *Fat10* mRNA and protein expression were recorded. Choi and colleagues showed that *Fat10* mRNA was induced within 3 h of combined stimulation and peaked at 12–15 h in comparison to single stimulation. In that study, FAT10 protein became visible by 6 h of TNF-α/IL-6 stimulation and the expression was maintained till 30 h post combined stimulation (Choi et al., 2014). In our experimental set-up, we cultured bulk T cells and B cells that were sorted magnetically from mouse splenocytes (Fig. 6B) or human PBMCs (Fig. 6C) with 400 U/mL of TNF-α and IL-6 for 24 h. The untreated samples were incubated for 24 h and *Fat10* mRNA induction of treated samples was measured relative to the untreated samples. Interestingly, apart from bulk T cells from mouse splenocytes, none of the tested immune cell subsets showed enhanced *fat10* expression upon TNF-α/IL-6 stimulation. This further confirmed that *fat10* expression is optimally and synergistically induced by specifically combining TNF-α and IFN-γ at least in T and B cells (Liu et al., 1999; Raasi et al., 1999; Schregle et al., 2018).

In summary, we could show that *fat10* mRNA was up-regulated upon LCMV and IAV infection. FAT10$^{-/-}$ splenocytes have an impaired ability to secrete IFN-γ while they produce enhanced levels of type I IFNs. It hence appears that FAT10 fine tunes the interferon responses to viral infection by counter-regulating type I and type II interferons.

Acknowledgements

We thank the personnel of the animal facility of Konstanz University for animal care taking and the staff of the flow cytometry facility of the University of Konstanz (FlowKon) for help with flow cytometry. This work was supported by the German Research Foundation (DFG) Collaborative Research Center SFB969, project C01. The authors declare no conflicts of interest.

Appendix A. Supplementary data

Supplementary material related to this article can be found, in the online version, at doi:https://doi.org/10.1016/j.molimm.2019.02.010.

References

Aichem, A., Groettrup, M., 2016. The ubiquitin-like modifier FAT10 in cancer development. Int. J. Biochem. Cell Biol. 79, 451–461.
Aichem, A., Pelzer, C., Lukasiak, S., Kalveram, B., Sheppard, P.W., Rani, N., Schmidtke, G., Groettrup, M., 2010. USE1 is a bispecific conjugating enzyme for ubiquitin and FAT10, which FAT10ylates itself in cis. Nat. Commun. 1, 13.
Aichem, A., Kalveram, B., Spinnenhirn, V., Kluge, K., Catone, N., Johansen, T., Groettrup, M., 2012. The proteomic analysis of endogenous FAT10 substrates identifies p62/SQSTM1 as a substrate of FAT10ylation. J. Cell. Sci. 125, 4576–4585.
Basler, M., Lauer, C., Beck, U., Groettrup, M., 2009. The proteasome inhibitor bortezomib enhances the susceptibility to viral infection. J. Immunol. 183, 6145–6150.
Bates, E.E., Ravel, O., Dieu, M.C., Ho, S., Guret, C., Bridon, J.M., Ait-Yahia, S., Briere, F., Caux, C., Banchereau, J., Lebecque, S., 1997. Identification and analysis of a novel member of the ubiquitin family expressed in dendritic cells and mature B cells. Eur. J. Immunol. 27, 2471–2477.
Bitzer, A., Basler, M., Krappmann, D., Groettrup, M., 2017. Immunoproteasome subunit deficiency has no influence on the canonical pathway of NF-kappaB activation. Mol. Immunol. 83, 147–153.
Canaan, A., Yu, X., Booth, C.J., Lian, J., Lazar, I., Gamfi, S.L., Castille, K., Kohya, N., Nakayama, Y., Liu, Y.C., Eynon, E., Flavell, R., Weissman, S.M., 2006. FAT10/diubiquitin-like protein-deficient mice exhibit minimal phenotypic differences. Mol. Cell. Biol. 26, 5180–5189.
Canaan, A., DeFuria, J., Perelman, E., Schultz, V., Seay, M., Tuck, D., Flavell, R.A., Snyder, M.P., Obin, M.S., Weissman, S.M., 2014. Extended lifespan and reduced adiposity in mice lacking the FAT10 gene. Proc. Natl. Acad. Sci. U. S. A. 111, 5313–5318.
Choi, Y., Kim, J.K., Yoo, J.Y., 2014. NFkappaB and STAT3 synergistically activate the expression of FAT10, a gene counteracting the tumor suppressor p53. Mol. Oncol. 8, 642–655.
den Haan, J.M., Lehar, S.M., Bevan, M.J., 2000. CD8(+) but not CD8(-) dendritic cells cross-prime cytotoxic T cells in vivo. J. Exp. Med. 192, 1685–1696.
Fan, W., Cai, W., Parimoo, S., Schwarz, D.C., Lennon, G.G., Weissman, S.M., 1996. Identification of seven new human MHC class I region genes around the HLA-F locus. Immunogenetics 44, 97–103.
Farrar, M.A., Schreiber, R.D., 1993. The molecular cell biology of interferon-γ and its receptor. Annu. Rev. Immunol. 11, 571–611.
Frucht, D.M., Fukao, T., Bogdan, C., Schindler, H., O'Shea, J.J., Koyasu, S., 2001. IFN-gamma production by antigen-presenting cells: mechanisms emerge. Trends Immunol. 22, 556–560.
Gong, P.F., Canaan, A., Wang, B., Leventhal, J., Snyder, A., Nair, V., Cohen, C.D., Kretzler, M., DAgati, V., Weissman, S., Ross, M.J., 2010. The ubiquitin-like protein FAT10 mediates NF-kappa B activation. J. Am. Soc. Nephrol. 21, 316–326.
Herrmann, V.L., Hartmayer, C., Planz, O., Groettrup, M., 2015. Cytotoxic T cell vaccination with PLGA microspheres interferes with influenza A virus replication in the lung and suppresses the infectious disease. J. Control. Release 216, 121–131.
Hipp, M.S., Kalveram, B., Raasi, S., Groettrup, M., Schmidtke, G., 2005. FAT10, a ubiquitin-independent signal for proteasomal degradation. Mol. Cell. Biol. 25, 3483–3491.
Huang, S., Hendriks, W., Althage, A., Hemmi, S., Bluethmann, H., Kamijo, R., Vilcek, J., Zinkernagel, R.M., Aguet, M., 1993. Immune response in mice that lack the interferon-γ receptor. Science 259, 1742–1745.
Jin, J.P., Li, X., Gygi, S.P., Harper, J.W., 2007. Dual E1 activation systems for ubiquitin differentially regulate E2 enzyme charging. Nature 447, 1135–1137.
Kägi, D., Ledermann, B., Burki, K., Seiler, P., Odermatt, B., Olsen, K.J., Podack, E.R., Zinkernagel, R.M., Hengartner, H., 1994. Cytotoxicity mediated by T cells and natural killer cells is greatly impaired in perforin-deficient mice. Nature 369, 31–37.
Lee, C.G., Ren, J., Cheong, I.S., Ban, K.H., Ooi, L.L., Yong Tan, S., Kan, A., Nuchprayoon, I., Jin, R., Lee, K.H., Choti, M., Lee, L.A., 2003. Expression of the FAT10 gene is highly upregulated in hepatocellular carcinoma and other gastrointestinal and gynecological cancers. Oncogene 22, 2592–2603.
Liu, Y., Pan, J., Zhang, C., Fan, W., Collinge, M., Bender, J.R., Weissman, S.M., 1999. A MHC-encoded ubiquitin-like protein (FAT10) binds noncovalently to the spindle assembly checkpoint protein MAD2. Proc. Natl. Acad. Sci. U. S. A. 96, 4313–4318.
Lukasiak, S., Schiller, C., Oehlschlaeger, P., Schmidtke, G., Krause, P., Legler, D.F., Autschbach, F., Schirmacher, P., Breuhahn, K., Groettrup, M., 2008. Proinflammatory cytokines cause FAT10 upregulation in cancers of liver and colon. Oncogene 27, 6068–6074.
Merbl, Y., Refour, P., Patel, H., Springer, M., Kirschner, M.W., 2013. Profiling of ubiquitin-like modifications reveals features of mitotic control. Cell 152, 1160–1172.
Nguyen, K.B., Cousens, L.P., Doughty, L.A., Pien, G.C., Durbin, J.E., Biron, C.A., 2000. Interferon α/β-mediated inhibition and promotion of interferon-γ: STAT1 resolves a paradox. Nat. Immunol. 1, 70–76.
Oldstone, M.B., Ahmed, R., Byrne, J., Buchmeier, M.J., Riviere, Y., Southern, P., 1985. Virus and immune responses: lymphocytic choriomeningitis virus as a prototype model of viral pathogenesis. Br. Med. Bull. 41, 70–74.
Orange, J.S., Biron, C.A., 1996. An absolute and restricted requirement for IL-12 in natural killer cell IFN-γ production and antiviral defense. J. Immunol. 156, 1138–1142.
Ou, R., Zhou, S.H., Huang, L., Moskophidis, D., 2001. Critical role for alpha/beta and gamma interferons in persistence of lymphocytic choriomeningitis virus by clonal exhaustion of cytotoxic T cells. J. Virol. 75, 8407–8423.
Pelzer, C., Kassner, I., Matentzoglu, K., Singh, R.K., Wollscheid, H.-P., Scheffner, M., Schmidtke, G., Groettrup, M., 2007. UBE1L2, a novel E1 enzyme specific for ubiquitin. J. Biol. Chem. 282, 23010–23014.

Pfaffl, M.W., Horgan, G.W., Dempfle, L., 2002. Relative expression software tool (REST) for group-wise comparison and statistical analysis of relative expression results in real-time PCR. Nucl. Acids Res. 30, e36.
Raasi, S., Schmidtke, G., de Giuli, R., Groettrup, M., 1999. A ubiquitin-like protein which is synergistically inducible by interferon-γ and tumor necrosis factor-α. Eur. J. Immunol. 29, 4030–4036.
Raasi, S., Schmidtke, G., Groettrup, M., 2001. The ubiquitin-like protein FAT10 forms covalent conjugates and induces apoptosis. J. Biol. Chem. 276, 35334–35343.
Ren, J., Kan, A., Leong, S.H., Ooi, L.L., Jeang, K.T., Chong, S.S., Kon, O.L., Lee, C.G., 2006. FAT10 plays a role in the regulation of chromosomal stability. J. Biol. Chem. 281, 11413–11421.
Ren, J., Wang, Y., Gao, Y., Mehta, S.B., Lee, C.G., 2011. FAT10 mediates the effect of TNF-alpha in inducing chromosomal instability. J. Cell. Sci. 124, 3665–3675.
Ross, M.J., Wosnitzer, M.S., Ross, M.D., Granelli, B., Gusella, G.L., Husain, M., Kaufman, L., Vasievich, M., D'Agati, V.D., Wilson, P.D., Klotman, M.E., Klotman, P.E., 2006. Role of ubiquitin-like protein FAT10 in epithelial apoptosis in renal disease. J. Am. Soc. Nephrol. 17, 996–1004.
Schmidtke, G., Aichem, A., Groettrup, M., 2014. FAT10ylation as a signal for proteasomal degradation. Biochim. Biophys. Acta 1843, 97–102.
Schregle, R., Mah, M.M., Mueller, S., Aichem, A., Basler, M., Groettrup, M., 2018. The expression profile of the ubiquitin-like modifier FAT10 in immune cells suggests cell type-specific functions. Immunogenetics 70, 429–438.
Sen, G.C., 2001. Viruses and interferons. Annu. Rev. Microbiol. 55, 255–281.
Spinnenhirn, V., Farhan, H., Basler, M., Aichem, A., Canaan, A., Groettrup, M., 2014. The ubiquitin-like modifier FAT10 decorates autophagy-targeted Salmonella and contributes to Salmonella resistance in mice. J. Cell. Sci. 127, 4883–4893.
Suarez-Ramirez, J.E., Tarrio, M.L., Kim, K., Demers, D.A., Biron, C.A., 2014. CD8 T cells in innate immune responses: using STAT4-dependent but antigen-independent pathways to gamma interferon during viral infection. mBio 5, e01978–01914.
Teijaro, J.R., Ng, C., Lee, A.M., Sullivan, B.M., Sheehan, K.C., Welch, M., Schreiber, R.D., de la Torre, J.C., Oldstone, M.B., 2013. Persistent LCMV infection is controlled by blockade of type I interferon signaling. Science 340, 207–211.
van den Broek, M.F., Muller, U., Huang, S., Aguet, M., Zinkernagel, R.M., 1995. Antiviral defense in mice lacking both alpha/beta and gamma interferon receptors. J. Virol. 69, 4792–4796.
Wilson, E.B., Yamada, D.H., Elsaesser, H., Herskovitz, J., Deng, J., Cheng, G., Aronow, B.J., Karp, C.L., Brooks, D.G., 2013. Blockade of chronic type I interferon signaling to control persistent LCMV infection. Science 340, 202–207.
Zhang, Y., Tang, J., Yang, N., Liu, Q., Zhang, Q., Zhang, Y., Li, N., Zhao, Y., Li, S., Liu, S., Zhou, H., Li, X., Tian, M., Deng, J., Xie, P., Sun, Y., Lu, H., Zhang, M.Q., Jin, N., Jiang, C., 2016. FAT10 is critical in influenza A virus replication by inhibiting type I IFN. J. Immunol. 197, 824–833.